

A Comparison between Heterogeneous and Homogeneous Gas Flow Model in Slurry Bubble Column Reactor for Direct Synthesis of DME

Sadegh Papari, Mohammad Kazemeini, and Moslem Fattahi

Abstract—In the present study, a heterogeneous and homogeneous gas flow dispersion model for simulation and optimisation of a large-scale catalytic slurry reactor for the direct synthesis of dimethyl ether (DME) from syngas and CO₂, using a churn-turbulent regime was developed. In the heterogeneous gas flow model the gas phase was distributed into two bubble phases: small and large, however in the homogeneous one, the gas phase was distributed into only one large bubble phase. The results indicated that the heterogeneous gas flow model was in more agreement with experimental pilot plant data than the homogeneous one.

Keywords—Modelling, Slurry bubble column, Dimethyl ether synthesis, Homogeneous gas flow, Heterogeneous gas flow

I. INTRODUCTION

DME has a wide-range of applications including; as a liquefied petroleum gas (LPG) substitute, transportation fuel, propellant, chemical feedstock and fuel cell [1]. Reactions associated with the single-stage process for DME production may be divided into the following steps:

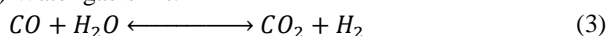
i) Methanol synthesis:



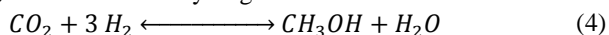
ii) Methanol dehydration:



iii) Water gas-shift:



iv) Carbon dioxide hydrogenation:



Syngas to DME conversion is easier and more efficient to perform in a simple slurry reactor.

This enables; i) maintenance of a uniform temperature throughout the reactor, which is important for highly exothermic reactions; ii) easy addition and removal of catalyst to the reaction medium and iii) good temperature control, which prevents catalyst sintering [2].

Although a 5 and 100 tons/day slurry pilot plant was built in Japan, no commercial-scale syngas to DME conversion has been reported to date [3] and literature on the simulation and design of industrial DME synthesis reactors is very limited.

Therefore, in the current study, a mathematical model utilising homogeneous and heterogeneous hydrodynamics model was developed and compared to pilot plant experimental data available in the literature. Then, the effects of temperature and pressure on the CO conversion as well as; DME production, and optimum values of the feed gas composition and reactor dimensions were investigated. In this model energy balance was ignored because the temperature of the slurry reactor utilising cooling water tubes was taken to be constant which indeed is the case.

II. MODELLING

The mathematical model for description of the homogeneous as well as; heterogeneous gas flow based upon dispersion model for three-phase (*i.e.*; small bubbles, large bubbles and slurry phase) and catalyst particle sedimentation are presented in Table I.

S. Papari is with the Department of Chemical and Petroleum Engineering, Sharif University of Technology, Azadi Avenue, P.O. Box 11365-9465, Tehran, Iran (e-mail: sadegh65papari@yahoo.com).

M. Kazemeini is with the Department of Chemical and Petroleum Engineering, Sharif University of Technology, Azadi Avenue, P.O. Box 11365-9465, Tehran, Iran (corresponding author to provide phone: +98-21-6616-5425; fax: +98-21-6602-2853; e-mail: kazemini@sharif.edu).

M. Fattahi is with the Department of Chemical and Petroleum Engineering, Sharif University of Technology, Azadi Avenue, P.O. Box 11365-9465, Tehran, Iran (e-mail: moslemfattahi@che.sharif.edu).

TABLE I
MODEL EQUATION FOR HOMOGENEOUS AND HETEROGENEOUS GAS FLOW MODEL IN SLURRY BUBBLE COLUMN

| <i>Homogeneous gas flow mathematical model</i> | <i>Heterogeneous gas flow mathematical model</i> |
|--|---|
| <i>Mass balance for Gas phase</i> | <i>Mass balance for Large-bubbles phase</i> |
| $\frac{\partial}{\partial z} \left[\epsilon_G E_G \frac{\partial C_{j,G}}{\partial z} \right] - \frac{\partial (U_G C_{j,G})}{\partial z} - k_1 a (C_j^* - C_{j,SL}) = 0$ | $\frac{\partial}{\partial z} \left[\epsilon_{LB} E_{LB} \frac{\partial C_{j,LB}}{\partial z} \right] - \frac{\partial (U_{LB} C_{j,LB})}{\partial z} - k_1 a_{LB} (C_j^* - C_{j,SL}) = 0$ |
| <i>Mass balance for slurry phase</i> | <i>Mass balance for Small-bubbles phase</i> |
| $\begin{aligned} \frac{\partial}{\partial z} \left[(1 - \epsilon_G) E_{SL} \frac{\partial C_{j,SL}}{\partial z} \right] - \frac{\partial (U_{SL} C_{j,SL})}{\partial z} \\ + k_1 a_{LB} (C_j^* - C_{j,SL}) \\ + k_1 a_{sb} (C_j^* - C_{j,SL}) + (1 \\ - \epsilon_G) \sum_{i=1}^{N_r} M_{cat} v_{j,i} r_i = 0 \end{aligned}$ | $\frac{\partial}{\partial z} \left[\epsilon_{SB} E_{SB} \frac{\partial C_{j,SB}}{\partial z} \right] - \frac{\partial (U_{SB} C_{j,SB})}{\partial z} - k_1 a_{SB} (C_j^* - C_{j,SL}) = 0$ |
| <i>Mass balance for particles</i> | <i>Mass balance for slurry phase</i> |
| $\frac{\partial}{\partial z} \left[(1 - \epsilon_G) E_S \frac{\partial C_S}{\partial z} \right] - \frac{\partial}{\partial z} [(1 - \epsilon_G) U_P - U_{SL}) C_S] = 0$ | $\begin{aligned} \frac{\partial}{\partial z} \left[(1 - \epsilon_G) E_{SL} \frac{\partial C_{j,SL}}{\partial z} \right] - \frac{\partial (U_{SL} C_{j,SL})}{\partial z} + k_1 a_{LB} (C_j^* - C_{j,SL}) \\ + k_1 a_{sb} (C_j^* - C_{j,SL}) + (1 \\ - \epsilon_G) \sum_{i=1}^{N_r} M_{cat} v_{j,i} r_i = 0 \end{aligned}$ |
| <i>Boundary condition in the inlet of column</i> | <i>Mass balance for particles</i> |
| $U_G C_{j,G} - \epsilon_G E_G \frac{\partial C_{j,G}}{\partial z} = U_G C_{j0}$ | $\frac{\partial}{\partial z} \left[(1 - \epsilon_G) E_S \frac{\partial C_S}{\partial z} \right] - \frac{\partial}{\partial z} [(1 - \epsilon_G) U_P - U_{SL}) C_S] = 0$ |
| $U_{SL} C_{j,SL} - (1 - \epsilon_G) E_{SL} \frac{\partial C_{j,SL}}{\partial z} = 0$ | <i>Boundary condition in the inlet of column</i> |
| $(1 - \epsilon_G) E_S \frac{\partial C_S}{\partial z} + ((1 - \epsilon_G) U_P - U_{SL}) C_S + U_{SL} C_{ave} = 0$ | $U_{LB} C_{j,LB} - \epsilon_{LB} E_{LB} \frac{\partial C_{j,LB}}{\partial z} = U_{LB} C_{j0}$ |
| <i>Boundary condition in the outlet of column</i> | $U_{SB} C_{j,SB} - \epsilon_{SB} E_{SB} \frac{\partial C_{j,SB}}{\partial z} = U_{SB} C_{j0}$ |
| $\frac{\partial C_{j,G}}{\partial z} = 0, \frac{\partial C_{j,SL}}{\partial z} = 0, \frac{\partial C_S}{\partial z} = 0$ | $U_{SL} C_{j,SL} - (1 - \epsilon_G) E_{SL} \frac{\partial C_{j,SL}}{\partial z} = 0$ |
| | $(1 - \epsilon_G) E_S \frac{\partial C_S}{\partial z} + ((1 - \epsilon_G) U_P - U_{SL}) C_S + U_{SL} C_{ave} = 0$ |
| | <i>Boundary condition in the outlet of column</i> |
| | $\frac{\partial C_{j,LB}}{\partial z} = 0, \frac{\partial C_{j,SL}}{\partial z} = 0, \frac{\partial C_{j,SB}}{\partial z} = 0, \frac{\partial C_S}{\partial z} = 0$ |

The empirical correlations of gas hold up, volumetric mass transfer coefficient, superficial gas velocity of small bubbles, hindered sedimentation velocity of particles, dispersion coefficient of small, large bubble, liquid, slurry velocity and gas solubility in paraffin liquid for prediction of the DME production and CO conversion in a large-scale slurry bubble column reactor were obtained from references available in the literature [4-13].

In the present study, kinetics of the methanol synthesis, Carbon dioxide hydrogenation and DME synthesis as independent reactions were taken from the work of Liu *et al.* [3] provided as follows:

$$r_{CO} = A_1 \exp\left(-\frac{A_2}{RT}\right) f_{CO}^{A_3} f_{H_2}^{A_4} \left(1 - \frac{f_M}{K_{f_1} f_{CO} f_{H_2}^2}\right) \quad (5)$$

$$r_{CO_2} = A_5 \exp\left(-\frac{A_6}{RT}\right) f_{CO}^{A_7} f_{H_2}^{A_8} \left(1 - \frac{f_M f_w}{K_{f_2} f_{CO_2} f_{H_2}^3}\right) \quad (6)$$

$$r_D = A_9 \exp\left(-\frac{A_{10}}{RT}\right) f_M^{A_{11}} \left(1 - \frac{f_w f_D}{K_{f_3} f_M^2}\right) \quad (7)$$

III. RESULTS AND DISCUSSION

The reactor operating conditions were listed in Table 2. The mathematical model was solved by the MATLAB software 2010a.

Fig. 1 indicated the parity of CO conversion and DME production for comparing the two hydrodynamic models (*i.e.* homogeneous vs. heterogeneous) with experimental pilot plant data [14]. It might be seen from this figure that the prediction of the plant data for heterogeneous gas flow model was more accurate than that of the homogeneous one and the average relative deviations (ARD) of the former was lower than the latter one. The heterogeneous model predicted that the CO conversion and DME production with ARD of 6.35% and 4.65%; respectively. Hence, in this paper for investigation of the effects of operating parameters the heterogeneous gas flow model was utilized.

Fig. 2 illustrated the effect of temperature on CO conversion and DME productivity in a large-scale bubble column slurry reactor. It is seen that the increasing temperature led to the enhancement of the CO conversion and DME productivity due to the fact that increasing temperature accelerated methanol synthesis, CO hydrogenation and methanol dehydration reactions. In addition, at higher temperatures the mass transfer coefficient and the solubility of the syngas in the slurry phase increased which meant the mass transfer resistance was lowered. However, it is reminded that the temperature may reach to limited heights due to the fact that all reactions in the direct DME synthesis were exothermic. Furthermore, at higher temperatures sintering phenomenon might have occurred which in turn could have resulted in reduced catalytic activity. Considering all these together, it is clear from this figure that the optimum value for the operating temperature was chosen to be 265°C.

Fig. 3 showed the effect of pressure on the CO conversion and DME production. As results indicated the increasing operating pressure resulted in improvement of CO conversion and DME productivity. The enhanced performance of the reactor might have been interpreted in terms of the carbon dioxide and methanol synthesis being mole-reducing reactions. Besides, the water gas shift and DME synthesis reactions had similar number of moles on both sides of reactions. Therefore, the increased operating pressure had positive effect on the CO conversion and DME production. Furthermore, the increased operating pressure led to enhancement of the mass transfer area which followed by increased volumetric mass transfer coefficient. Although increased pressure corresponded to the improved reactor performance, running reactions at high pressures was also limited by high operating costs. Therefore, a pressure of 50bars was selected as the optimum operating pressure for the direct DME synthesis.

Ultimately, results of homogeneous versus heterogeneous phase for prediction of the optimum values of reactor dimensions and feed gas composition were similar. The optimum value of reactor diameter and height were thus, determined to be 3.2 and 20 meters; respectively and the best feed gas composition $\left(\frac{H_2-CO_2}{CO+CO_2}\right)$ for maximum conversion obtained to be 2.

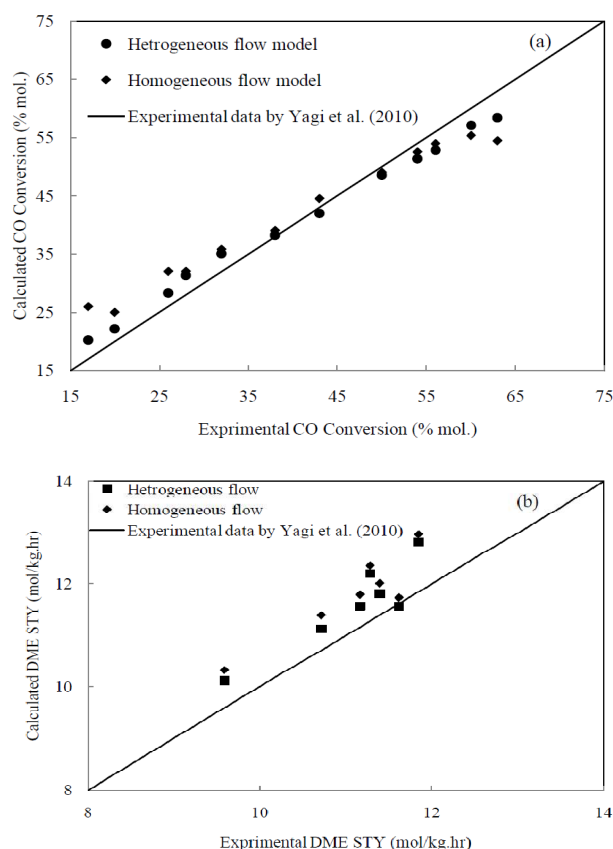


Fig. 1 A comparison between homogeneous and heterogeneous dispersion model with experimental pilot plant

TABLE II
OPERATING CONDITION OF BUBBLE COLUMN SLURRY REACTOR

| Volume of reactor | Temperature range | Pressure range | Superficial gas velocity | Mass of catalyst | Mass of paraffin | Feed gas composition $\frac{H_2 - CO_2}{CO + CO_2}$ | Number of cooling pipes |
|--------------------|-------------------|----------------|--------------------------|------------------|------------------|--|-------------------------|
| 160 m ³ | 240-265°C | 4-6 Mpa | 0.22 $\frac{m}{s}$ | 34.46 ton | 68 ton | 1-2 | 400 (38 mm) |

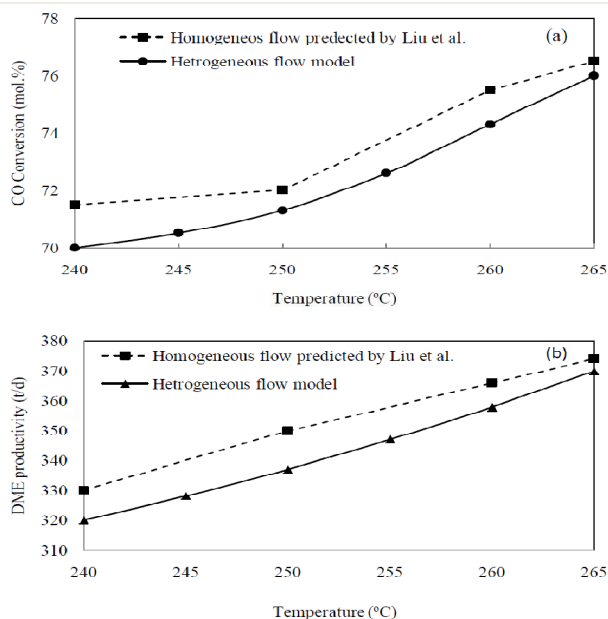


Fig. 2 CO conversion and DME productivity vs. temperature: P = 6 Mpa, W/F = 11 (g-cat.hr/mol), $\epsilon_s = 0.33$ wt. %, $U_G = 0.22$ m/s

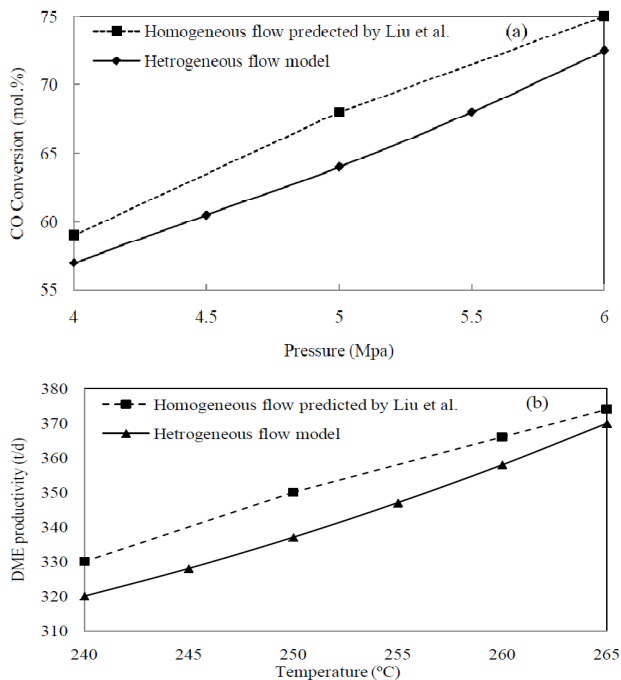


Fig. 3 CO conversion and DME productivity vs. pressure: T=260°C, W/F = 11 (g-cat.hr/mol), $\epsilon_s = 0.33$ wt. %, $U_G = 0.22$ m/s

IV. CONCLUSIONS

In the present study, homogeneous and heterogeneous gas flow models were compared to experimental pilot plant data. It was concluded that the heterogeneous model was more accurate for prediction of such plant information. Then effects of pressure and temperature on the CO conversion and DME productivity in a large-scale bubble column slurry reactor were investigated and the optimum values for these operating conditions suggested. Moreover, the results showed no difference between homogeneous and heterogeneous models for prediction of optimum values of the feed gas composition and reactor dimensions.

REFERENCES

- [1] K. L. Ng, D. Chadwick, and B. A. Toseland, "Kinetics and modelling of dimethyl ether synthesis from synthesis gas," *Chem. Eng. Sci.*, vol. 54, pp. 3587-3592, 1999.
- [2] Z. Chen, H. Zhang, W. Ying, and D. Fang, "Study on direct alcohol/ether fuel synthesis process in bubble column slurry reactor," *Fron. Chem. Eng. Chin.*, vol. 4, pp. 461-471, 2010.
- [3] D. Liu, X. Hua, and D. Fang, "Mathematical Simulation and Design of Three-Phase Bubble Column Reactor for Direct Synthesis of Dimethyl Ether from Syngas," *J. Nat. Gas Chem.*, vol. 16, pp. 193-199, 2007.
- [4] C. Maretto, and R. Krishna, "Modelling of a bubble column slurry reactor for Fischer-Tropsch synthesis," *Catal. Today*, vol. 52, pp. 279-289, 1999.
- [5] C. Maretto, and R. Krishna, "Design and optimisation of a multi-stage bubble column slurry reactor for Fischer-Tropsch synthesis," *Catal. Today*, vol. 66, pp. 241-248, 2001.
- [6] I. G. Reilly, D. S. Scott, T. J. W. Debruijn, and D. Macintyre, "A role of gas phase momentum in determining gas holdup and hydrodynamic flow regimes in bubble column operations," *Can. J. Chem. Eng.*, vol. 72, pp. 3-12, 1994.
- [7] R. Krishna, and J. W. A. de Swart, J. Ellenberger, G. B. Martina, and C. Maretto, "Gas holdup in slurry bubble columns: effect of column diameter and slurry concentrations," *AIChE J.*, vol. 43, pp. 311-316, 1997.
- [8] D. J. Vermeer, and R. Krishna, "Hydrodynamics and mass transfer in bubble columns operating in the churn-turbulent regime," *Ind. Eng. Chem. Process Des. Dev.*, vol. 20, pp. 475-482, 1981.
- [9] D. N. Smith, and J. A. Ruether, "Dispersed solid dynamics in a slurry bubble column," *Chem. Eng. Sci.*, vol. 40, pp. 741-775, 1985.
- [10] J. W. A. De Swart, R. E. van Vliet, and R. Krishna, "Size, structure and dynamics of "large" bubbles in a two-dimensional slurry bubble column," *Chem. Eng. Sci.*, vol. 51, pp. 4619-4629, 1996.
- [11] R. W. Field, and J. F. Davidson, "Axial dispersion in bubble columns," *Trans. Inst. Chem. Eng.*, vol. 58, pp. 228-235, 1980.
- [12] W.-D. Deckwer, A. Schumpe, "Improved tools for bubble column reactor design and scale-up," *Chem. Eng. Sci.*, vol. 48, pp. 889-911, 1993.
- [13] T. Wang, and J. Wang, "Numerical simulations of gas-liquid mass transfer in bubble columns with a CFD-PBM coupled model," *Chem. Eng. Sci.*, vol. 62, pp. 7107-7118, 2007.

- [14] H. Yagi, Y. Ohno, N. Inoue, K. Okuyama, and S. Aoki, "Slurry Phase Reactor Technology for DME Direct Synthesis," *Int. J. Chem. Reactor Eng.*, vol. 8, pp. A109, 2010.

NOMENCLATURE

| | |
|----------------------|--|
| r_{CO}, r_{CO_2} | Intrinsic kinetics rate of carbon monoxide, carbon dioxide and dimethyl ether (mol/(hr.g-cat)) |
| r_D | Reactor height (m) |
| L | Reactor diameter (m) |
| D_R | Operating pressure (Mpa) |
| P | Reaction temperature (K) |
| T | Gas constant ($\frac{J}{mol.K}$) |
| R | Molar concentration of j component in large bubble phase (mol/m ³) |
| $C_{j, LB}$ | Molar concentration of j component in small bubble phase (mol/m ³) |
| $C_{j, SB}$ | Molar concentration of j component in slurry phase (mol/m ³) |
| $C_{j, SL}$ | Catalyst concentration (kg/m ³) |
| C_S | Equilibrium molar concentration in liquid (mol/m ³) |
| C_j^* | Volumetric mass transfer coefficient for large bubbles (1/s) |
| $(k_1 a)_{LB}$ | Volumetric mass transfer coefficient for small bubbles (1/s) |
| $(k_1 a)_{SB}$ | Rate constant of methanol synthesis |
| k_{f1} | Rate constant of carbon dioxide hydrogenation |
| k_{f2} | Rate constant of methanol dehydration |
| k_{f3} | Partial pressure of CO, (Mpa) |
| P_{CO} | Partial pressure of H ₂ , (Mpa) |
| P_{H_2} | Partial pressure of CO ₂ , (Mpa) |
| P_{CO_2} | Partial pressure of methanol, (Mpa) |
| P_M | Partial pressure of water, (Mpa) |
| P_w | Mass of catalyst (kg) |
| M_{cat} | Superficial velocity of large bubbles (m/s) |
| U_{LB} | Superficial velocity of small bubbles (m/s) |
| U_{SB} | Superficial velocity of slurry phase (m/s) |
| U_{SL} | Inlet superficial velocity of slurry phase (m/s) |
| U_{SL} | Superficial gas velocity (m/s) |
| U_G | Inlet superficial gas velocity (m/s) |
| U_{G0} | Hindered sedimentation velocity (m/s) |
| U_P | Diffusion coefficient (m ² /s) |
| D_j | Large bubble dispersion coefficient (m ² /s) |
| E_{LB} | Small bubble dispersion coefficient (m ² /s) |
| E_{SB} | Slurry phase dispersion coefficient (m ² /s) |
| E_{SL} | |
| <i>Greek symbols</i> | |
| ε_{SB} | Small bubbles gas holdup |
| ε_G | Total gas holdup |
| ε_{LB} | Large bubbles gas holdup |
| ε_S | Solid concentration |
| ν_{ij} | Reaction coefficient |